Wearable Haptic Array of Flexible Electrostatic Transducers

Ian Trase[1], Hong Z. Tan[2], Zi Chen[1], and John X. J. Zhang[1(✉)]

[1] Thayer School of Engineering, Dartmouth College, 14 Engineering Drive, Hanover, NH 03755, USA
john.zhang@dartmouth.edu
[2] School of Electrical and Computer Engineering at Purdue University, West Lafayette, IN 47907, USA

Abstract. We demonstrate a wearable flexible electrostatic transducer (FET) matrix that conforms to the skin and can be used to generate complex haptic signals. The transducers consist of a pair of flexible electrodes that are attracted based on electrostatic force. We designed and built a 2 by 2 matrix of transducers from a pair of flexible films, with the design optimized for indentation into the skin. A transducer with a 10 mm by 10 mm footprint and a height of 2 mm effectively generated perceptible stimulus on the skin when operated at 150 V–250 V. Three psychophysical experiments were carried out to evaluate the properties of the new device as a wearable haptic display. Experiment 1 showed that the matrix of transducers was able to linearly boost perceived intensity when compared to a single transducer. Experiment 2 indicated that it was possible to indistinguishably replicate multi-frequency signals delivered to one transducer using multiple transducers that each operated at one of the frequencies. In Experiment 3, four movement-based stimulation patterns were designed using tactile illusion, and the identification rates were significantly above chance level. Our findings demonstrate that the compact, flexible, and scalable transducer array is well suited as a new type of actuator for wearable haptics research and applications.

Keywords: Haptics · Transducer · Electrostatic · Flexible electrodes · Sensing · Wearable

1 Introduction

Wearable haptic technology is found in a variety of consumer devices, generally using linear resonant actuators (LRAs) or eccentric rotary motors (ERMs). These technologies generate vibrations at one or more frequencies that can be perceived on the skin. While small and efficient, these technologies are rigid and lack the ability to deliver complex signals over a wide frequency range. Other methods of haptic actuation include piezoelectric actuation and voice coils, but these have higher voltage or power consumption requirements. There is a need for flexible and compact haptic actuator arrays that can conform to the skin and deliver complex signals over a wide frequency and intensity ranges.

Haptic arrays have been developed for a variety of applications. Tactile sensing "skins" for robots are a current area of research using both triboelectric [1] and piezoelectric films [2]. These skins seek to sense a broad range of frequencies while still retaining flexibility. As most tactile sensing technologies are reversible (especially piezoelectric systems), these designs provide insight into actuation array systems as well. Both research and commercial activities are being conducted with ultrasonic transduction arrays that can generate sensation remotely in air, away from the array itself. Most current research uses piezoelectric printed polymer membranes (PPTs) to achieve actuation [3, 4], but work has also been done with thin flexible electrostatic actuators [5]. Arrays have been shown integrated into a wirelessly charged and controlled device on the skin [6], and work on soft piezoelectrics has also been conducted [7].

Significant research has been conducted into the use of haptic actuator arrays to generate tactile sensations, either through direct skin contact or through remote ultrasonic transduction in air. Haptic arrays can take advantage of several important psychophysical properties of the skin to deliver rich sensations. A key parameter when designing haptic arrays is the two-point discrimination threshold [8], which describes the distance at which two stimuli on the skin are indistinguishable from a single stimulus. This threshold is often quite large, for example on the order of 30–40 mm on the forearm [9]. An array of haptic transducers needs to have an inter-actuator spacing above this threshold for the delivered stimuli to be perceived as separate events. Haptic arrays with spacing below the two-point threshold can deliver complex stimuli that are perceived as a single, richer stimulus. Most day-to-day haptic events fall into this second category. By carefully designing stimuli, the total amount of information transferred can be increased [10]. We can exploit this effect to generate several well-known haptic illusions, including the apparent motion effect [11]. In this phenomenon, a series of discrete stimuli are perceived as a single stimulus moving smoothly across the surface of the skin. Through effects like this, an array can be used to generate smooth signals from a relatively sparse array of discrete systems, though still below the two-point discrimination distance. Algorithms have been generated to optimize this sensation, including the Tactile Brush algorithm [12] and the algorithm developed by Park et al. [13].

We developed a wearable haptic array based on our previous research into flexible electrostatic transducers [14, 15]. The transducers consist of a flexible buckled electrode bonded to an unbuckled electrode with an air gap in between. When an alternating voltage is applied across the two electrodes, they move closer and farther apart to generate perceivable vibration. The flexible and buckled nature of the electrodes makes them resistant to pull-in and able to operate at large length scales compared to the electrostatic force distance [16, 17]. The transducers can operate at a range of frequencies while under a variety of strain conditions, making them well-suited for conformal operation on the skin. These transducers were integrated into a two by two array that allowed for independent control of each tactor (tactile stimulator). The shape and response of the transducer elements were verified using COMSOL.

From a perception point of view, a transducer array opens new opportunities for delivering stimuli that are more complex than those possible with a single transducer. For example, two or more tactors can generate signals that are perceived to be more intense than the maximum intensity possible with a single tactor, thereby extending the

achievable intensity range [18]. In terms of the waveforms used to drive tactors, many haptic applications call for stimuli with rich spectral contents in order to achieve a large set of distinct stimuli (e.g., [19–21]). Since it is generally more difficult to develop broad bandwidth tactors than to develop resonant-type tactors with tunable resonant frequencies, it is desirable to use two nearby tactors each driven at a single frequency to emulate the sensation of a stimulus containing more than one frequency components. Finally, it has also been shown that movement-based stimuli are highly effective at increasing the information transmission achievable with haptic interfaces [22]. More than one tactor is needed in order to generate tactile movement illusions [11]. To assess the efficacy of using the transducer array to deliver complex stimuli, three psychophysical experiments were conducted to test (1) whether simultaneously activating multiple tactors can lead to a perceivable increase in stimulus intensity, (2) the perceptual difference between a single tactor driven by a signal with two frequency components and two tactors each driven at one frequency, and (3) the distinctiveness of four simulated movement patterns generated by the tactor array. The present research explores the development of a new, flexible haptic array for wearable applications. This array was characterized through theory and simulation, as well as through a psychophysical study. The results verify that the array can be used to deliver a rich range of tactile stimuli while still being comfortable and conformal to the skin.

2   Device Design and Characterization

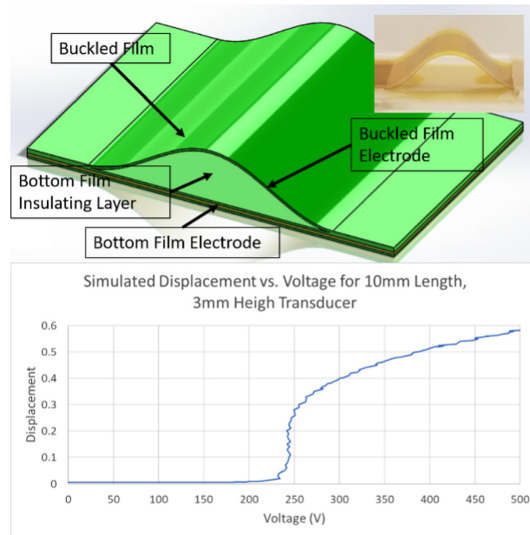### 2.1   Electromechanical Theory

Fig. 1. A) Schematic of individual flexible electrostatic transducer. Inset: photograph of example transducer. B) Simulated voltage-displacement curve for a 10 mm × 10 mm transducer, with turn-on voltage at 240 V.

Each transducer is composed of a pair of thin films that have been coated with a gold electrode on one side. The film that goes in contact with the skin, shown in Fig. 1A, is buckled such that the point of maximum extension presses into the skin. The other film remains flat and undergoes only minor curvature when deformed against the skin. The buckled film is coated with the gold electrode on the side facing the flat film, while the electrode of the flat film is fully encased within that film's multiple layers. Thus, the buckled film begins in a prestressed state while the flat film begins in a relaxed state. When a voltage is applied between the two electrodes, a Coulombic attraction force is generated between the two films. For the voltages and geometry of the device in question, this electrostatic force is negligible for most of the length of the buckled film. However, the force becomes very high at points where the film separation is low. This includes both the region where the two films are in constant contact, as well as the point at which the buckled film begins to leave the flat film. The high force felt at this point is enough to move the buckled film closer to the flat film by an incremental amount. This motion further moves the point of film contact, allowing for increased force at a new location. This positive feedback loop continues until the downward pressure from the electrostatic force is balanced by restoring pressure from the bending force of the buckled film. The approximate governing equations for this relationship can be found in [14, 15], but the phenomena has no closed-form solution and is best studied through simulation. Figure 1B shows an example voltage-displacement curve. Here we can see the characteristic "turn-on" voltage of the transducer, as well as the relatively flat displacement response. These properties make the FET act as a pseudo-binary actuator, with an on state, an off state, and a narrow region where voltage has a very large effect on displacement.
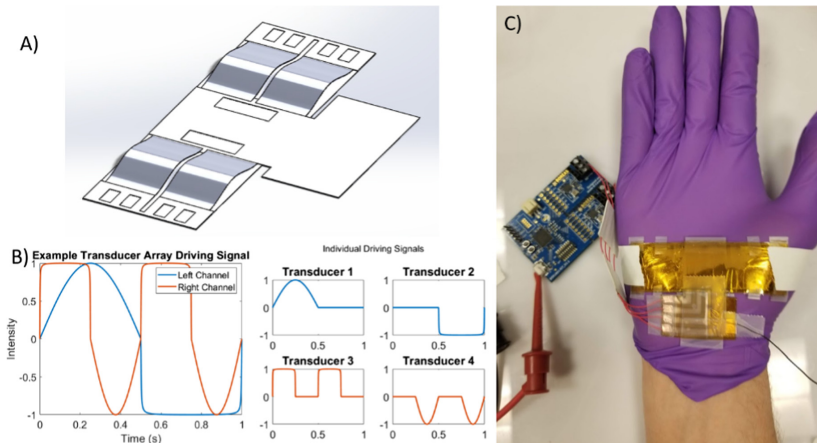
2.2 Device Design

Fig. 2. A) Schematic of transducer array. B) Example waveform used to drive array, with components separated out for clarity. C) Photograph of electrical setup for transducer array, showing Boreas 1901 development kit with array on palm, ready for psychophysical experiment.

A basic schematic of the transducer array is shown in Fig. 2A. The array is composed of two composite films that have been laser-cut and bonded into place. The top buckled film consists of a piece of 25 μm thick Kapton film coated with a 40 nm thick layer of gold as an electrode. This film begins as a single piece of Kapton film that was then laser-cut by a Laser Pro Spirit GLS into the prescribed shape. An acrylic mask 1/16" thick was then placed over the cut Kapton, and 20 nm of gold was sputter-coated onto the film. The top film features gold traces that lead away from the center of the device and off to the side. These traces lead to wire interconnects, which need to be moved away from the transducers to maintain the low profile and conformal nature of the device. The bottom film begins as a lightly prestretched piece of 2.5 μm thick Mylar film taped on its edges to a glass slide. Another acrylic mask was used to help deposit a 20 nm thick layer of gold to the Mylar. A ~ 5 μm thick layer of 20:3 base to curing agent PDMS is then spin coated onto the Mylar, and the composite is then cured at 70 °C for 2 h. After 1 h, a laser-cut piece of Kapton film is adhered to the PDMS, and the Mylar-Gold-PDMS-Kapton composite is excised from the glass slide using a razorblade at the end of 2 h. The two films are then aligned such that the gold-coated side of the top film and the Mylar side of the bottom film are facing each other. They are bonded using tape at a series of prescribed locations, such that each of the four transducers in the top film buckles into a precise shape and the two films maintain good contact everywhere else. In this configuration, the two electrodes are separated only by the 2.5 μm Mylar film, which allows for large electric fields at low applied voltages. The ultimate product is a two by two array, in which each transducer has a footprint of 10 mm by 10 mm.

The top film has four separate gold electrodes, each connected to a separate wire. These wires are connected to the four terminals of a Boreas 1901 Development Kit. This development kit consists of a pair of BOS1901 piezoelectric drivers with a microchip allowing it to be used as a USB audio device. Each driver is capable of supplying anywhere from 0 V to 95 V to either of two channels, though only one channel may be active at a given time. Using this configuration, all four transducers on the flexible array can be controlled using a single audio signal from a computer or any device capable of providing USB audio. The left stereo channel controls one pair of transducers, while the right channel controls the other pair. Within each channel, the positive component of the audio signal controls one transducer while the negative component controls the other. An image of the Boreas Kit connected to the flexible array with an inset of the general waveform shape is shown in Fig. 2B. The bottom film electrode was connected through a wire to the powered terminal of a Trek Model 2210 high voltage amplifier controlled through a Keysight 33522B signal generator and isolated using a Triad Magnetics MD-250-E medical grade isolation transformer. The high voltage amplifier was used to provide a DC bias of –150 V to the bottom electrode, allowing the voltage differential across each transducer to range from 150 V to 245 V. As the displacement-vs-voltage response of the flexible transducers is highly nonlinear, applying a bias voltage increases the change in the displacement generated by the Boreas chip. This effect is shown through experiment and simulation in Fig. 3A and B. The relationship between displacement and voltage at –150 V is used to calibrate the decibel change of the signals during the psychophysical experiments.
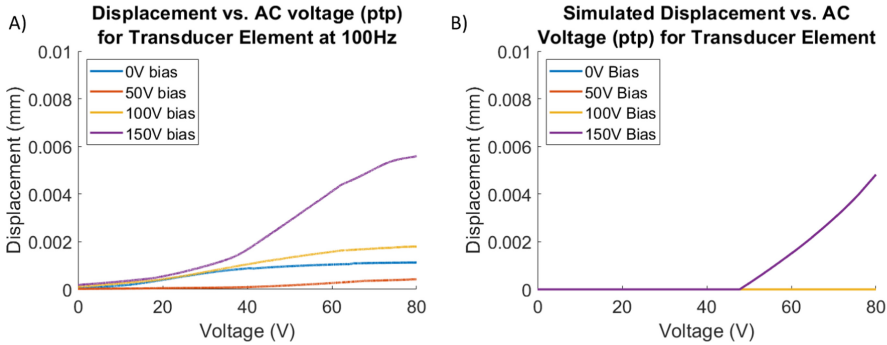
Fig. 3. A) Experimental displacement-voltage curves for an individual transducer on the array at different DC biases. B) Simulated displacement-voltage curves for the same set of parameters.

To experimentally determine the displacement of the transducer at different voltage and frequency conditions, a PDV-100 laser vibrometer was used. The vibrometer was set up such that the laser was illuminating the point of maximum extension on the buckled film. The analog vibrometer signal was then collected by a MATLAB program using a National Instruments USB-4431 DAQ, converted to a displacement signal, and correlated with the driving signal generated by the Boreas Kit. For the linear vibrometer test, a series of signals at frequencies from 1 Hz to 2000 Hz with linearly ramping amplitudes from 0 V to 80 V over 5 s were tested. Each signal was tested for 4 separate DC biases from the high voltage amplifier: 0 V, –50 V, –100 V, and –150 V. The voltage-displacement relationship of the transducers is highly nonlinear, and thus receives a significant benefit from the DC offset generated by the high voltage amplifier. This effect was also observed in user testing, in which participants could not feel vibration even at the maximum amplitude unless the bias was set to –150 V. Experiment and simulations were also conducted to understand the frequency response of the transducers. It was desired for the transducers to have large displacements from 0 to 500 Hz, as this is the frequency range of interest for most haptic stimulation. Figure 4A and B show that the transducer has a reasonably large response in the desired range, and a flat frequency dependence at lower frequencies. Lastly, we conducted simulations to explore the restoring force and actual displacement that the transducer exerted on the skin when actuating, summarized in Fig. 4C and D. For this data, the skin and the device were both approximated as connected springs with prescribed natural lengths and spring constants. The spring constant of the transducer is highly nonlinear, as the shape of the transducer changes significantly as it is compressed, so the force-displacement relationship was directly simulated in COMSOL. The results were used to build a function to describe the spring constant of the transducer at a given displacement. Human skin is a complicated mechanical system, and a wide range of elasticities have been reported for it. Skin has significant viscoelastic properties and responds differently to different displacement magnitudes and frequencies. For this analysis, we simplified elasticities in the reported range to get a sense for the potential response. As such, the results should be viewed as an approximate estimate of the interface at the skin and device.
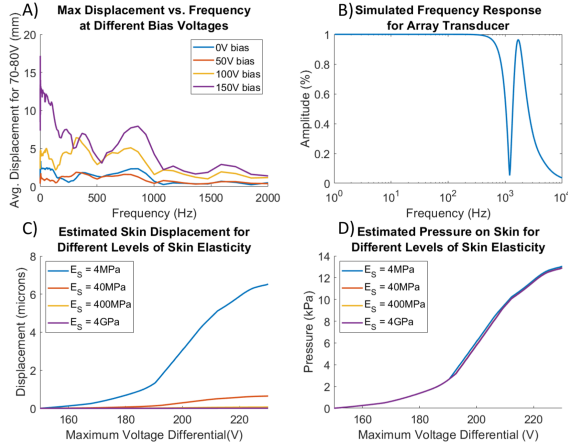
Fig. 4. A) Experimental displacement-frequency curves for a single transducer on the array at different bias voltages, showing a strong resonance around 800 Hz. B) Simulated frequency response for the transducer, showing a flat response until around 800 Hz. C) Estimated skin displacement by device for different skin elasticities. D) Estimated pressure on skin by device for different skin elasticities.

2.3 Characterization

A variety of experiments were conducted on the fabricated transducer array to determine relationships between displacement, voltage, and frequency, as well as the effects of crosstalk, noise, and complex signals. The results are shown in detail in the sections below.
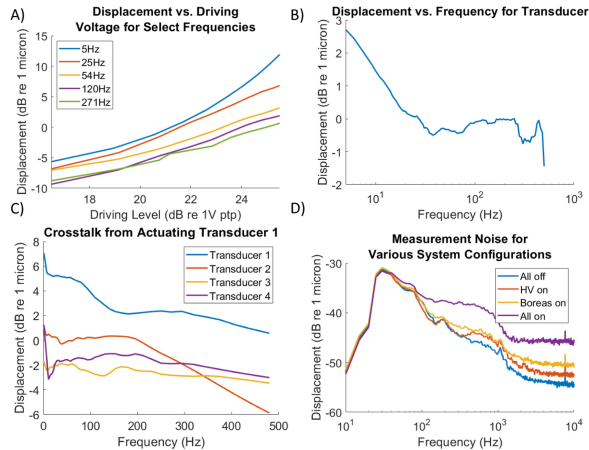

Fig. 5. Experimental displacement data for transducer array. A) Displacement vs. driving voltage for select frequencies. B) Example displacement-frequency curve at 330 V input level. C) Crosstalk levels as a function of frequency when transducer 1 is driven at 330 V. D) Measurement noise for different electrical configurations.

A laser vibrometer was used to measure the displacement of the four transducers in the array for different driving conditions. In a basic test, the displacement was measured for a parametric array of voltage and frequency conditions, and the results are summarized in Fig. 5A and B. The first figure shows how the displacement increases with driving level as expected, with higher frequencies providing lower levels of displacement at all driving levels. The second figure shows a characteristic displacement-frequency curve for a given voltage, displaying a characteristic drop-off in displacement intensity as the frequency increases, with a relatively flat region in the area of interest from ~20 Hz–300 Hz.

Figure 5C shows the results from a crosstalk test, where a single transducer (#1) was driven and the displacement of the undriven transducers was measured. We can see that the displacement of the undriven transducers was lower but still significant. The graph shows displacement differences ranging from a difference of around 8 dB at low frequencies to 4 dB at high frequencies. This significant crosstalk can be attributed to the reasonably high level of connectivity between the 4 transducers. All the buckled transducer films are fabricated from a single piece of Kapton film, and kirigami-style cuts are made to create the 4 buckled films. Since the transducers are not mechanically isolated from each other, small vibrations (on the order of 1 μm or less) can travel laterally through the film to generate vibrations in the other transducers. It is expected that at higher displacement levels, the dB difference between the driving transducer and the other transducers would be much lower. In addition, better mechanical isolation between the transducers should further reduce the crosstalk. For example, fully separating the buckled film during manufacturing will reduce crosstalk significantly.

Figure 5D summarizes results from tests conducted to determine the noise floor of the transducers under various electrical conditions. The transducer array is connected on one end to a high voltage amplifier controlled by a signal generator, and on the other end to a piezo driver driven by a desktop PC. Both of these components are a source of noise, as is the natural environment. Tests were conducted with both electrical pieces on, one on and the other off, and both off. The displacement was again measured with a laser vibrometer. The results are in line with what was expected, with all electronics on producing the most noise and all off producing the least. It was initially expected that the amplifier would be a source of more noise than the piezo driver due to the amplifier's higher power draw and voltages, but this was not the case. It may be that the noise from the PC passed through the piezo driver is larger than the amplifier noise. In addition, the sum of the independent noise from the amplifier and the driver was smaller than the noise when both were used together, indicating that there is potential interference between the two. In any case, these results indicate that the magnitude of the noise is much lower than even the lowest displacements achievable through driving the transducers.

Figure 6 explores the results of various frequency-based experiments. In Fig. 6A, the phase difference between the pre-amplified driving signal and the measured displacement is compared. It is very clear that the relationship is based on linear phase, which can be attributed to the effect of the high voltage amplifier. The transducer acts as a capacitor in-circuits, and thus one would expect its phase delay to be highly nonlinear. A linear phase indicates that the transducer suffers from very little phase delay, and in general the electronics used to drive the devices contributed more to the delay than the transducer

itself. Similarly, Fig. 6B describes the group delay for various voltages, which is a low constant. This is again due to the high voltage amplifier, but the levels are low enough not to be a concern for the target frequency range.
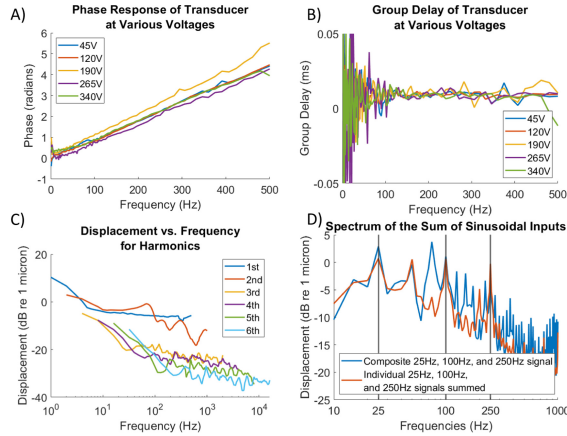

Fig. 6. Frequency analysis of transducer array. A) Phase difference between the pre-amplified driving signal and the measured displacement. B) Group delay of the transducer array for a selection of driving voltages. C) Analysis of higher harmonics for transducer array. D) Comparison of multispectral driving signal outputs.

Figure 6C explores the amplitude of higher harmonics when the transducer is driven at a frequency. The graph makes it clear that the higher-order harmonics (3rd and up) are greatly diminished compared to the fundamental and 2nd frequencies. For a few frequencies, the 2nd harmonic is even larger than the base frequency. This is expected behavior, as the transducer acts as a partial frequency-doubling system. The force experienced by the transducer is roughly proportional to the square of the voltage. Because of this, both the positive and negative portions of the driving sinusoids have the same effect, and the frequency is effectively doubled. Thus, we would expect to see similar levels for the first two frequencies, and lower levels thereafter.

Figure 6D examines the ability of the transducer array to reproduce signals composed of multiple base frequencies. The three frequencies used for the psychophysical evaluation were chosen as inputs (25 Hz, 100 Hz, and 250 Hz). Each frequency was played alone at a low amplitude to eliminate clipping, and the results were recorded. A signal composed of all three frequencies playing at once, each at the same amplitude as in the solo test, was then used to drive the transducer and the results recorded. The three solo frequency results were then summed and compared to the combined signal results, as shown in the figure. If the spectrum of the two signals matched exactly, it would indicate that the transducer was able to perfectly add frequencies together with no distortion. We can see that the results are quite similar, and the levels of the three frequencies in question are almost identical. The combined signal, however, suffers from increased amplitude at all the harmonics of the 25 Hz signal. This indicates that the

summation of signals is nonlinear and may be because the relationship between voltage and displacement in the transducer is nonlinear to begin with.

3   Psychophysical Evaluation

We conducted three psychophysical experiments to determine the efficacy of the transducer array at delivering haptic stimuli to the skin. In the first experiment, the ability of the transducer array to generate higher perceived intensity levels than a single tactor was studied. In the second experiment, the participants discriminated between a stimulus produced by one tactor that contained two frequency components, and another stimulus produced by two separate tactors each driven at one of the two frequencies. The final experiment measured the ability of the transducer array to deliver four distinct haptic signals using a tactile movement illusion.

3.1   Methods

Participants. Ten participants (5 females, age 22–33 years old) took part in each of the three experiments. No participant suffered from any known sensorimotor deficiency. The participants gave their informed consent to the protocol approved by Dartmouth College's Institutional Review Board (IRB). They were compensated for their time.

Apparatus. A transducer array was mounted to the palm of the dominant hand, as shown in Fig. 2C. Each participant wore a nitrile glove sized such that the glove was slightly tight but not constricting by self-report. The glove served as an insulating failsafe in case the Kapton film suffered an electrical breakdown and it may reduce the perceptibility of vibrations on the skin. The participant rested their hand lightly on a table with the palm and device facing down. The array was mounted to the palm such that the buckled film was facing inwards, and the flexible film conformed to the skin. This caused each transducer to be lightly compressed. When a voltage is applied the buckled film is pulled away from the skin and the pressure on the skin is reduced. The bottom film of the array was connected to a high voltage amplifier controlled by a signal generator that provided a –150 V DC bias. Each of the four transducers in the buckled array was connected to a different terminal in the Boreas Kit driven by a PC, such that they could be independently controlled. A MATLAB program delivered audio signals to the Boreas chip, and the experimenter used the program to record each participant's responses. All participants wore headphones to prevent sound from the FET being used as audio cues.

Procedure. Prior to the three experiments, the perceived intensities of the four transducers were calibrated in two steps following the methods described by Reed et al. [19]. It has been shown that the equal-sensation contours for vibrotactile perception are mostly parallel in decibel scale for touch [23]. Therefore, the perceived stimulus intensity can be specified by calculating the ratio of the driving voltage over that at the human detection threshold in dB scale (called dB sensation level, or dB SL). The detection threshold was measured for each participant on a single transducer (the reference transducer) using a 3-interval, 2-alternative, 1-up 3-down adaptive forced-choice procedure [24]. On each trial, the participant received three stimulus intervals. One randomly selected interval

contained a 500-ms signal at 100 Hz, while the other 2 intervals were empty. The timing of the 3 intervals were indicated visually through an LED on the Boreas kit and the inter-interval gap was kept at 500 ms. The participant's task was to indicate during which of the 3 intervals a signal was felt. The voltage was decreased after 3 consecutive correct responses and increased after 1 incorrect response. The threshold obtained with this transformed up-down method corresponds to the 79.4% point on the psychometric function [25]. The adaptive procedure continued until 8 reversals had been obtained. A reversal is defined as the voltage changing from decreasing to increasing, or vice versa. The voltage changed by 5 dB for the first 2 reversals for faster convergence, and by 2 dB for the remaining 6 reversals for better resolution of the estimated thresholds. The local maxima and minima at the last 6 reversals were averaged to get an estimate of the threshold. In the second step, the relative intensities of the four tactors were calibrated using a method of adjustment [24]. For each of the 3 non-reference tactors (target tactor), the participant felt 3 100-Hz vibrations: the first on the reference tactor, the second on the target tactor, and the third on the reference tactor again. The reference signal was always at 10 dB SL. The participant was asked to respond whether the target signal felt stronger or weaker than the reference signal. The target signal voltage was adjusted in 2-dB steps until the participant indicated that the reference and target signals were equally intense. The dB measurements for all tests were measured in terms of the equivalent zero-load displacement at that voltage. Thus, a 10 dB signal had $\sqrt{10}\times$ the displacement (as measured by a laser vibrometer) of a 0 dB SL signal, but not necessarily $\sqrt{10}\times$ the driving voltage amplitude. With the individual thresholds and adjustment values for the 3 target tactors, it was then possible to assign voltage multipliers for all four tactors to ensure that all participants felt all four tactors at desired intensities specified in dB SL during the subsequent experiments. These voltage multipliers were also used for the 25 Hz and 250 Hz signals, as the perceived intensity at different frequencies was assumed to be the same as dB SL [23].

Experiment 1: The difference in perceived intensities between single-transducer actuation and multi-transducer actuation was studied in a 1-interval, 4-alternative forced-choice identification experiment [24]. All signals were 500 ms in duration and 10 dB SL in intensity. Each participant completed 3 blocks (at 25 Hz, 100 Hz or 250 Hz, in a randomly assigned order) of 40 trials for a total of 120 trials. Before each block of 40 trials, the participant felt the 4 signals, one each with 1, 2, 3 and 4 transducers actuating simultaneously. For the signals with 1, 2, or 3 tactors, the actuated transducers were randomly chosen on each trial so as not to associate the number of actuated tactors with their locations. On each trial, one of the stimulus alternatives was chosen by randomization with replacement, and the participant indicated the perceived intensity by responding with an integer between 1 and 4. Trial-by-trial correct-answer feedback was provided. The first 10 trials in each 40-trial block were discarded to avoid training effect, and the remaining 30 trails were analyzed.

Experiment 2: The perceptual difference between two sinusoidal signals delivered via two tactors (each following a single-frequency input) and one tactor was studied in a 1-interval, 2-alternative forced-choice signal detection experiment. We hypothesized that the two signals would be indistinguishable due to the inability of the somatosensory system to assign a frequency to a particular spatial location when two tactors are located

within the two-point discrimination threshold. There were three experimental conditions involving different combinations of frequencies: 25 Hz and 100 Hz, 25 Hz and 250 Hz, and 100 Hz and 250 Hz. All signals were 500 ms in duration. Each participant completed 3 blocks (in a randomly assigned order) of 40 trials for a total of 120 trials. Prior to each condition, the perceived intensities of the two stimulus alternatives were equalized using a method of adjustment. The participant first felt two tactors each being driven at one of the frequencies (Signal A in Fig. 7A), then a single tactor being driven by the sum of the two single-frequency signals (Signal B in Fig. 7B), and back to the two tactors. Once again, the tactors were randomly selected for each presentation. The voltage of the stronger signal (the two-tactor signal that was presented first and last) was set at 10 dB SL. The voltage for the weaker signal (the one-tactor signal in the middle) was adjusted until the single-tactor and two-tactor signals felt equally intense. During each 40-trial block, the two stimulus alternatives were labeled signal 1 and 2 and the participants were not informed of the nature of the two signals. On each trial, the participant felt one of the two stimuli that was selected by randomization with replacement and responded "1" or "2".
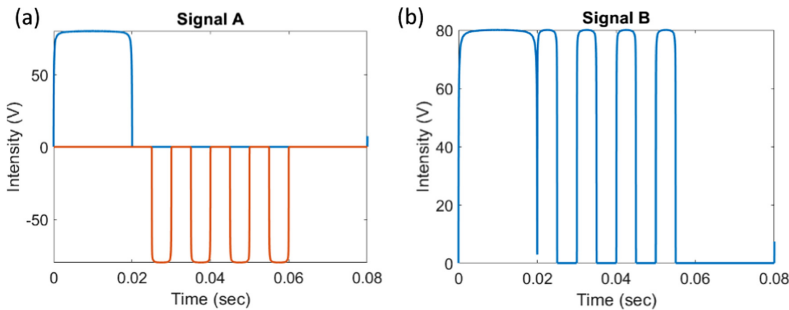

Fig. 7. A) Single period of signals sent to the two tactors for Signal A. B) Single period of signal sent to a single tactor for Signal B.

Experiment 3: The distinctiveness of movement patterns generated by the 2-by-2 tactor matrix was studied in a 1-interval, 4-alternative forced-choice identification experiment. The participant was shown a visual representation of four movement patterns: leftwards, rightwards, (clockwise) circular, and Z-shaped. The qualitative sketches of the perceived patterns are shown in Fig. 8. Prior to the experiment, the participants familiarized themselves with the patterns. The tactors were driven at 100 Hz at approximately 15 dB SL. On each trial, one of the four patterns was presented using randomization with replacement. The participant identified the pattern verbally which was recorded by the experimenter. Trial-by-trial correct-answer feedback was provided, and a total of 60 trials were collected per participant.

Data Analysis. The data from Experiment 1 were organized into 4-by-4 stimulus-response confusion matrices with the four rows corresponding to the number of tactors driven simultaneously, and the four columns the perceived intensity levels. There were a total of 30 confusion matrices for 10 participants and 3 frequencies. The data from the 10
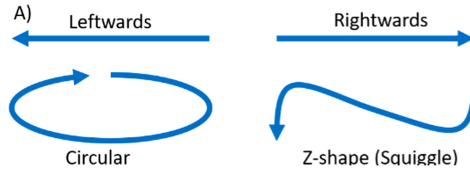
Fig. 8. A) qualitative perception of the four stimuli for experiment 3.

participants were then pooled at each frequency, resulting in three confusion matrices, one for each frequency. Percent-correct scores and information transfer were calculated from the three matrices (see [21]). For Experiment 2, the results were organized into 30 2-by-2 matrices with the rows corresponding to stimulus A and B and the columns the corresponding responses. The results were analyzed using signal detection theory to compute the sensitivity index d', a measure that is independent of response bias (see [24]). The d' scores from all 10 participants at the same frequency pair were then averaged, resulting in a total of three d' scores for the three experimental conditions. In general, a d' of above 1 indicates that the two signals are reliably distinguishable. The data from Experiment 3 were analyzed in the same manner as in Experiment 1.

3.2 Results and Discussion

Experiment 1: Figure 9 shows that the 4 levels of intensity are somewhat distinguishable, even with very limited training. The error patterns for all frequencies show that almost all errors are off by one, i.e. the participant was almost always close to the correct value. The overall percent-correct was 44% for the 25 Hz frequency, 50% for 100 Hz, 54% for 250 Hz, and 49% in aggregate. The overall error rate appeared frequency dependent, with the 25 Hz signals being more difficult to identify than the 100 Hz and 250 Hz signals. When information transfer was calculated, the values ranged from 0.47 bits at 25 Hz to 0.74 bits at 250 Hz. This means that even though the participants were able to discriminate the perceived intensities in a pairwise manner, they were unable to identify the four intensity levels. While it is theoretically possible for each transducer on the array to assume any intensity on a continuous distribution, it seems as though 4 levels are challenging for a user to identify. Indeed, 25 Hz signal is probably better suited to 2-3 intensity levels than to 4. Using multiple tactors to replicate different intensity levels can be useful when the tactor in question has a low dynamic range, or when the dynamic range is high, but the band of possible inputs is narrow and vulnerable to quantization error. In either of these cases, it may be better to use multiple transducers, each with only a few possible intensity values (or a single intensity value) to replicate the effect of a single transducer capable of taking on an infinite set of intensity values. While most transducers today fall into the latter category, that capability is unnecessary since a human cannot discriminate more than a few intensity values.

Experiment 2: The sensitivity indices for each configuration is summarized in Table 1, with the "All" row containing the average of the absolute values of the d's. the average standard deviation of d' was found to be $\sigma_{d'} = 0.41$.
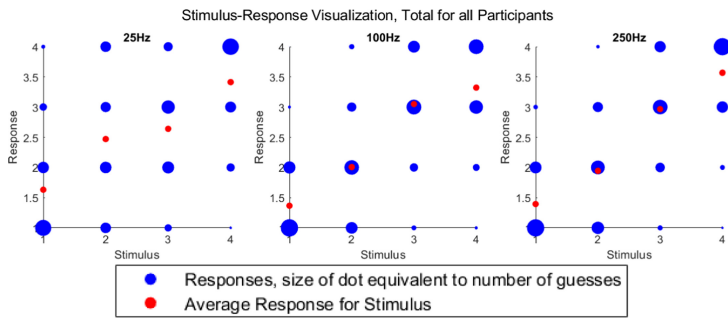
Fig. 9. Stimulus-response matrix visualization for intensity perception experiment. The red dots indicate the average response for each stimulus, while the blue dots indicate the total number of responses per stimulus, with larger dots indicating more responses. (Color figure online)

Table 1. Summary of d' values for combined frequency experiment.

Condition	d'	$\sigma_{d'}$	t-test
25 Hz & 100 Hz	0.40	0.41	1
25 Hz & 250 Hz	0.43	0.41	0
100 Hz & 250 Hz	0.47	0.41	0
All	0.44	0.41	1

By observing Table 1, it is clear that the d' values for all three configurations were below 1.0, indicating that the participants were unable to discriminate between two tactors each vibrating at a single frequency and one tactor being driven by the sum of two sinusoidal frequencies. This was expected since the distance between the two tactors were below the two-point discrimination threshold on the skin. A pairwise t-test was conducted, and the results show that the hypothesis that the 25 Hz and 100 Hz signal tests were indistinguishable passed a standard t-test, but the other two signal tests did not. The results from Experiment 2 further indicate that it may be possible to use this phenomenon to separate mechanically distinct parts of a transducer array while preserving the ability to generate complex stimuli. For example, the transducers in the current array are broadband, with a relatively flat response from 0–500 Hz, but an array could be constructed in which each transducer in the 2-by-2 array is tuned to a different resonant frequency. An array so constructed would still be able to produce results indistinguishable from a single transducer generating a complex waveform – even though each transducer in that theoretical array would be mechanically incapable of producing that signal. This would allow for transducers to be constructed with a stronger signal operating at a lower voltage, since each could be tuned for a specific frequency.

Experiment 3: The overall correct response rate was 64%. These are summarized in Fig. 10. Figure 10 explores how well participants were able to identify the four patterns,

with some participants doing significantly better than others. An information transfer analysis was conducted on this data, showing that the average information transfer was 0.81 ± 0.33 bits (perfect transmission for this experiment would be 2 bits). More fine-tuned signals with a larger matrix should be able to increase the information transfer rate significantly. This study helps to confirm that the phantom tactile sensation [12] is functional even on a thin and flexible haptic matrix, and supports the idea that the other various tactile illusions will also function effectively on this device. Tactile illusions such as the phantom tactile sensation are important to be able to replicate on advanced haptic devices, as they provide increased design space for signal generation, as well as helping to create realistic sensations from relatively sparse arrays [21].
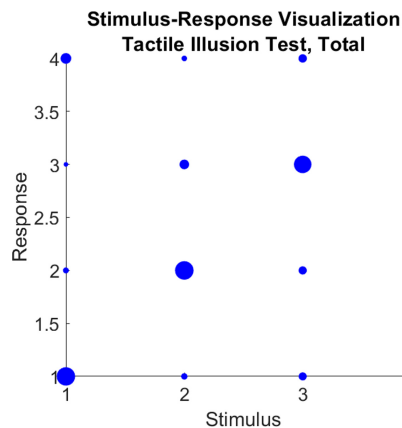

Fig. 10. Stimulus response visualization for the haptic illusion experiment. The blue dots indicate the total number of responses per stimulus, with larger dots indicating more responses. (Color figure online)

Qualitative sensation data were also collected through participant surveys at the end of each experiment. It was determined that no matter how many tactors were actuating, and no matter the signals being transduced, the device always presented to the wearer as a single stimulus point, rather than 1–4 discrete points. This is expected, as the transducer spacing is below the two-point discrimination threshold. When multiple tactors were actuated simultaneously, the phantom sensation illusion caused the single stimulus to appear to be in the middle of the two tactors as perceived by the participants, with the technical precise location governed by the relative intensity of the actuating tactors. Participants could tell when this phantom tactor moved in a certain direction but could not pinpoint its position on the skin. In other words, a phantom stimulus all the way to the right on the active array footprint followed by a stimulus in the middle felt qualitatively the same as a stimulus in the middle followed by a stimulus all the way to the left. The phantom sensation illusion also meant that certain experiments had trials that were not identical in sensation. For example, in the intensity perception experiment, a trial in which two tactors were actuated could in fact have any one of 6 tactor pairs. While this was unnoticed by the participants, this corresponds to 5 slightly different proximal stimuli (the two diagonal pairs both create a phantom tactor in the center of the device). It is

likely that the location movement reduced overall participant success rates by introducing distracting cues.

4   Concluding Remarks

We have designed, fabricated, and tested a functional array of flexible electrostatic transducers. The transducers can deliver perceptible vibration to the skin at a variety of frequencies. We conducted a suite of experimental tests and simulations to determine the expected displacement and force of the transducers. An array was fabricated from Kapton, Mylar, and gold electrodes. Three psychophysical experiments were conducted with 10 participants. It was found that multiple transducers could be used to boost the perceived intensity versus a single transducer. When measuring the perceived difference between a single transducer actuating at a combined frequency and a pair of transducers each actuating at a single frequency, it was found that there was no perceivable difference, indicating that the participants could not use spatial cues to identify signals. Finally, we showed that the participants could use the transducer array to identify haptic symbols from a set of four transducers with reasonable accuracy without any training. This collection of experiments and user studies shows that this transducer array has the potential to be used in advanced haptic devices to provide increased communication capabilities.

References

1. Zhou, K., et al.: Ultra-stretchable triboelectric nanogenerator as high-sensitive and self-powered electronic skins for energy harvesting and tactile sensing. Nano Energy **70**, 104546 (2020). https://doi.org/10.1016/j.nanoen.2020.104546
2. Seminara, L., et al.: Piezoelectric polymer transducer arrays for flexible tactile sensors. IEEE Sens. J. **13**(10), 4022–4029 (2013). https://doi.org/10.1109/JSEN.2013.2268690
3. van Neer, P.L.M.J., et al.: Feasibility of Using Printed Polymer Transducers for Mid-Air Haptic Feedback (2018)
4. van Neer, P., et al.: Development of a flexible large-area array based on printed polymer transducers for mid-air haptic feedback. 2019 Int. Congr. Ultrason. **38**, (2019). https://doi.org/10.1121/2.0001068
5. Kamigaki, T., Noda, A., Shinoda, H.: Thin and flexible airborne ultrasound phased array for tactile display. In: 2017 56th Annual Conference of the Society of Instrument and Control Engineers of Japan, SICE 2017, vol. 2017-Novem, pp. 736–739 (2017). https://doi.org/10.23919/sice.2017.8105623
6. Yu, X., et al.: Skin-integrated wireless haptic interfaces for virtual and augmented reality. Nature **575**(7783), 473–479 (2019). https://doi.org/10.1038/s41586-019-1687-0

7. Sorgini, F., et al.: Encapsulation of piezoelectric transducers for sensory augmentation and substitution with wearable haptic devices. Micromachines **8**(9) (2017). https://doi.org/10.3390/mi8090270

8. Craig, J.C., Johnson, K.O.: The two-point threshold: not a measure of tactile spatial resolution. Curr. Dir. Psychol. Sci. **9**(1), 29–32 (2000). https://doi.org/10.1111/1467-8721.00054

9. Nolan, M.F.: Two-point discrimination assessment in the upper limb in young adult men and women. Phys. Ther. **62**(0031-9023) (Print), 965–969 (1982). https://doi.org/10.1093/ptj/62.7.965

10. Novich, S.D., Eagleman, D.M.: Using space and time to encode vibrotactile information: toward an estimate of the skin's achievable throughput. Exp. Brain Res. **233**(10), 2777–2788 (2015). https://doi.org/10.1007/s00221-015-4346-1

11. Lederman, S.J., Jones, L.A.: Tactile and haptic illusions. IEEE Trans. Haptics **4**(4), 273–294 (2011). https://doi.org/10.1109/TOH.2011.2

12. Israr, A., Poupyrev, I.: Tactile Brush: drawing on skin with a tactile grid display. Conference on Human Factors in Computing Systems- Proceedings, pp. 2019–2028 (2011). https://doi.org/10.1145/1978942.1979235

13. Song, J., Zhang, Y., Zhang, H., Wang, D.: Rendering Moving Tactile Stroke on the Palm Using a Sparse 2D Array, vol. 9774, no. 37, pp. 229–239 (2016). https://doi.org/10.1007/978-3-319-42321-0

14. Trase, I., Xu, Z., Chen, Z., Tan, H., Zhang, J.X.J.: Thin-film bidirectional transducers for haptic wearables. Sens. Actuators A Phys. **303**, 111655 (2019). https://doi.org/10.1016/j.sna.2019.111655

15. Trase, I.H., Xu, Z., Chen, Z., Tan, H.Z., Zhang, J.X.J.: Flexible electrostatic transducers for wearable haptic communication. In: Proceedings of World Haptics Conference 2019 (2019) (p. submitted)

16. Jebens, R., Trimmer, W., Walker, J.: Microactuators for aligning optical fibers. Sens. Actuators **20**(1–2), 65–73 (1989). https://doi.org/10.1016/0250-6874(89)87103-3

17. Legtenberg, R., Gilbert, J., Senturia, S.D., Elwenspoek, M.: Electrostatic curved electrode actuators. J. Microelectromech. Syst. **6**(3), 257–265 (1997). https://doi.org/10.1109/84.623115

18. Bensmaïa, S., Hollins, M., Yau, J., Carolina, N., Hill, C., Carolina, N.: Vibrotactile intensity and frequency information in the pacinian system: a psychophysical model. Percept. Psychophys. **67**(5), 828–841 (2005)

19. Reed, C.M., et al.: A Phonemic-Based Haptic Display for Speech communication. IEEE Trans. Haptics **12**(1), 2–17 (2019)

20. Tan, H.Z., Durlach, N.I., Reed, C.M., Rabinowitz, W.M.: Information transmission with a multifinger tactual display. Percept. Psychophys. **61**(6), 993–1008 (1999). https://doi.org/10.3758/BF03207608

21. Tan, H.Z., Choi, S., Lau, F.W.Y., Abnousi, F.: Methodology for maximizing information transmission of haptic devices: a survey. Proc. IEEE **108**(6), 945–965 (2020). https://doi.org/10.1109/JPROC.2020.2992561

22. Park, G., Cha, H., Choi, S.: Transactions on haptics, and undefined 2018. Haptic Enchanters: Attachable and Detachable Vibrotactile Modules and Their Advantages (2018). https://ieeexplore.ieee.org

23. Verrillo, R.T., Fraioli, A.J., Smith, R.L.: Sensation magnitude of vibrotactile stimuli. Percept. Psychophys. **6**(6), 366–372 (1969). https://doi.org/10.3758/BF03212793

24. Jones, L.A., Tan, H.Z.: Application of psychophysical techniques to haptic research. IEEE Trans. Haptics **6**(3), 268–284 (2013). https://doi.org/10.1109/TOH.2012.74

25. Levitt, H.: Transformed up-down methods in psychoacoustics. J. Acoust. Soc. Am. **49**(2B), 467–477 (1971)